Broadband *Z*-scan characterization using a high-spectral-irradiance, high-quality supercontinuum

Mihaela Balu,[1] Lazaro A. Padilha,[1] David J. Hagan,[1,2] Eric W. Van Stryland,[1,2,*] Sheng Yao,[3] Kevin Belfield,[3] Shijun Zheng,[4] Stephen Barlow,[4] and Seth Marder[4]

[1]*CREOL and Florida Photonics Center of Excellence, The College of Optics and Photonics, University of Central Florida, 4000 Central Florida Boulevard, Orlando, Florida 32816-2700, USA*
[2]*Department of Physics, University of Central Florida, 4000 Central Florida Boulevard, Orlando, Florida 32816, USA*
[3]*Department of Chemistry, University of Central Florida, 4000 Central Florida Boulevard, Orlando, Florida 32816, USA*
[4]*Center for Organic Photonics and Electronics and School of Chemistry and Biochemistry, Georgia Institute of Technology, Atlanta, Georgia 30332-0400, USA*
**Corresponding author: ewvs@creol.ucf.edu*

Received August 28, 2007; revised November 1, 2007; accepted November 2, 2007; posted November 20, 2007 (Doc. ID 86904); published January 9, 2008

We generate a high-spectral-irradiance, high-quality continuum by weakly focusing femtosecond pulses in Kr gas. We use this continuum as a source for rapid *Z*-scan measurements of the degenerate nonlinear absorption spectrum and the associated dispersion of the nonlinear refraction in optical materials throughout the visible. We measure the degenerate two-photon absorption spectra and the dispersion of the nonlinear refractive index, n_2, of two well-characterized semiconductors (ZnSe and ZnS) as reference samples for our method, along with dilute solutions of organic materials. The latter materials demonstrate application of the technique to samples with lower nonlinearities. © 2008 Optical Society of America

OCIS codes: 190.4400, 300.6420.

1. INTRODUCTION

Recently we introduced a technique for rapid and broadband frequency degenerate measurements of nonlinear absorption (NLA) and nonlinear refraction (NLR) [1,2]. In this method, referred to as white-light continuum (WLC) *Z* scan, a WLC was used to replace the single wavelength source conventionally used in a *Z*-scan experiment. The WLC source used [1,2] was generated by focusing femtosecond pulses into a cell filled with deionized water. The spectral energy densities of the WLC generated in this way were sufficient for measuring samples with large nonlinear absorption and refraction coefficients, for example, semiconductors.

In this paper, we describe how the usefulness of the technique can be greatly expanded by increasing the spectral irradiance of the WLC source and applying it to a variety of materials (e.g., low concentration solutions of organic materials). We obtain this source by weakly focusing femtosecond pulses into a chamber filled with noble gas [3]. This apparently simple change allows us to simultaneously measure the NLA spectra and dispersion of NLR over the entire visible spectrum in only a few minutes each with automation.

We present results of two-photon absorption (2PA) and n_2 measurements of two well-characterized semiconductors ZnS and ZnSe [4–6] to check the validity of our technique over the entire spectrum of the continuum. We also show measurements of dilute solutions of organic dyes.

2. WHITE-LIGHT CONTINUUM GENERATION

The laser source we use for continuum generation is a Clark-MXR Ti:sapphire laser system producing ~0.7 mJ, ~150 fs, 775 nm pulses at a 1 kHz repetition rate. We weakly focus the pulses generated by this source into a chamber filled with noble gas. To optimize the generated WLC source, we used different focusing geometries (lenses with focal lengths between 30 and 200 cm), different noble gases (Ar, Kr, Xe) at different pressures, and chambers of different lengths (80, 125, and 180 cm). As we varied these different parameters, we were interested in optimizing the continuum stability, broadening, and spatial profile at all wavelengths and its spectral energy density. We used the maximum energy available from our Ti:sapphire laser measured to be 710 μJ in front of the chamber.

In the first experiments, an 80 cm long stainless steel chamber filled with Kr gas was used. The continuum generated using a 30 cm focal length lens was very unstable, i.e., the energy in the visible fluctuated wildly from pulse to pulse as the pressure was varied between 3 and 5 atm. As the diffraction length was increased by increasing the focal length of the focusing lens, the continuum became more stable. However, damage threshold to the chamber windows imposed a limit on the focal length used. We used longer chambers to be able to generate continuum by using lenses with focal lengths as long as 200 cm. If the

focal length was too long, fluctuations again began to appear. We found that focal lengths in the range of 100 to 150 cm were acceptable.

We used Ar, Kr, and Xe as nonlinear media for continuum generation. The nonlinearities of these gases were estimated in Ref. [7] to be $n_2/p = 9.8\times10^{-20}$ cm^2/W atm for Ar, 2.8×10^{-19} for Kr, and 8.2×10^{-19} for Xe. Although these values have not been determined for femtosecond pulses, the trend (larger values corresponding to larger atomic mass gases) seems to be consistent with our experimental observations. Thus, for the same input energy, for stable continuum generation a 6.4 atm pressure was necessary for Ar while the pressures required for Kr and Xe were 2.4 and 1.35 atm, respectively. We used each of these gases for each of the different chamber lengths and for the different focusing geometries mentioned above. We monitored the continuum generation spectrum, its stability and the spatial profile corresponding to different wavelengths in the continuum for each of these cases. We obtained similar results for each of the three gases used in terms of continuum stability, broadening, and spatial profile. Therefore, we decided to use only one of them in our further experiments. We chose Kr, given the lower pressure required for continuum generation compared to Ar. We chose not to use Xe because it is much more expensive than Kr.

The configuration that resulted in the best characteristics for the WLC is depicted in Fig. 1. This gives the best combination of stability, spectral width, and energy density and demonstrated the broadest spectral range of Gaussian spatial profiles. The chamber used was 125 cm long filled with Kr gas at 2.4 atm. The focal length, $f = 150$ cm, corresponds to a measured beam waist w_0, of 145 μm (HW1/e^2M of irradiance) and a diffraction length $z_0(z_0 = \pi w_0^2/\lambda)$ of approximately 8.5 cm.

The 710 μJ, 775 nm, 145 fs (FWHM in irradiance) pulses resulted in a peak power of 4.9 GW, which is above the critical power for self-focusing of 1.4 GW in Kr at 2.4 atm [7]. The corresponding beam irradiance at focus was $\sim10^{13}$GW/cm^2. The WLC energy throughput was ~95% (after taking into account the Fresnel reflections on the chamber windows).

Given that the peak power exceeds the critical power for self-focusing, it is probable that filamentation occurs within the chamber [8–10]. A detailed analysis inside the chamber could determine the nature and characteristics of the generated WLC. However, for the purpose of performing Z scans, it was sufficient to simply characterize and use the WLC beam as it exits the chamber.

Using this configuration, taking single-shot data acquired for different wavelengths (narrow bandpass filter in place), showed ~90% of the shots were in a ±10% energy window, while ~80% were in a ±5% energy window. This is quite satisfactory for performing Z scans.

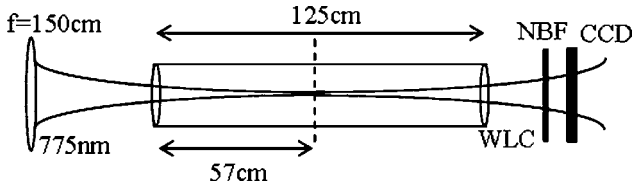

Fig. 1. Experimental configuration used for generating a stable, high-spectral-energy density, broadband, good spatial quality WLC source; NBFs are narrowband filters to monitor the beam spatial profile for different wavelengths of the WLC.

The continuum has a usable wavelength range from ~400 to 800 nm determined by the spectral irradiance and the spatial profiles. The WLC spectrum is shown in Fig. 2 with and without a notch filter to block the pump wavelength, which also rejects ranges centered around 530 and 400 nm. Although the WLC spectrum goes beyond 800 nm, the spatial profiles corresponding to wavelengths longer than 800 nm present a ring pattern. This behavior was observed for all the three gases and is actually predicted by numerical simulations [11]. While use of these wavelengths is possible, it would complicate the Z-scan analysis.

3. SPATIAL AND TEMPORAL CHARACTERIZATION OF FILTERED WHITE-LIGHT CONTINUUM WAVELENGTHS

To separate the WLC wavelengths for degenerate measurements, we use narrow bandwidth filters (NBFs, Corion Corp.) with ~8–12 nm FWHM, $\Delta\lambda/\lambda$ being constant to within ±15%. We notice a leakage of the pump wavelength through the NBFs close to 800 nm. For these wavelengths, we use a notch filter to block the pump. We characterize the transmitted beams both spatially and temporally over the range of 400–800 nm. The spatial profiles for several wavelengths in the continuum are shown in Fig. 3. The profiles are recorded by a CCD placed at 8 cm after the gas chamber. Energies within ~10 nm bandwidths, as obtained by transmission through the NBFs, are sufficient for NLA and NLR characterization (from a few nanojoules to hundreds of nanojoules).

To determine the pulse width for different wavelengths transmitted by the NBFs we use a commercial Grenouille setup for the NIR wavelengths [12] and interferometric and intensity autocorrelation measurements for the visible wavelengths. For the intensity autocorrelation we use 2PA as the nonlinear process (we use either a detector with a two-photon absorbing element, GaP, or ZnSe/ZnS placed in front of a Si detector) [13–15]. The interferomet-

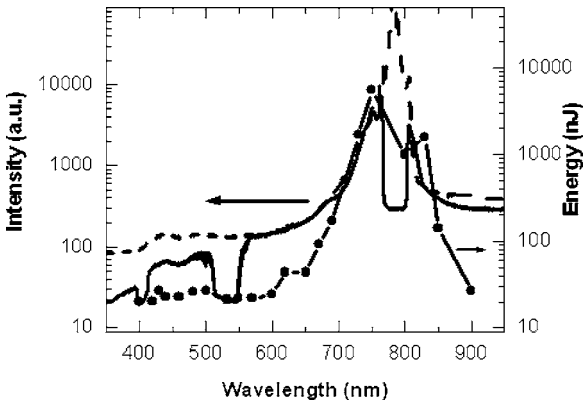

Fig. 2. White-light continuum spectrum before (dashed curve) and after (solid curve) a 780 nm notch filter. The black circles connected by a solid curve are the available energy for the Z scan after each narrowband filter (right vertical axis).

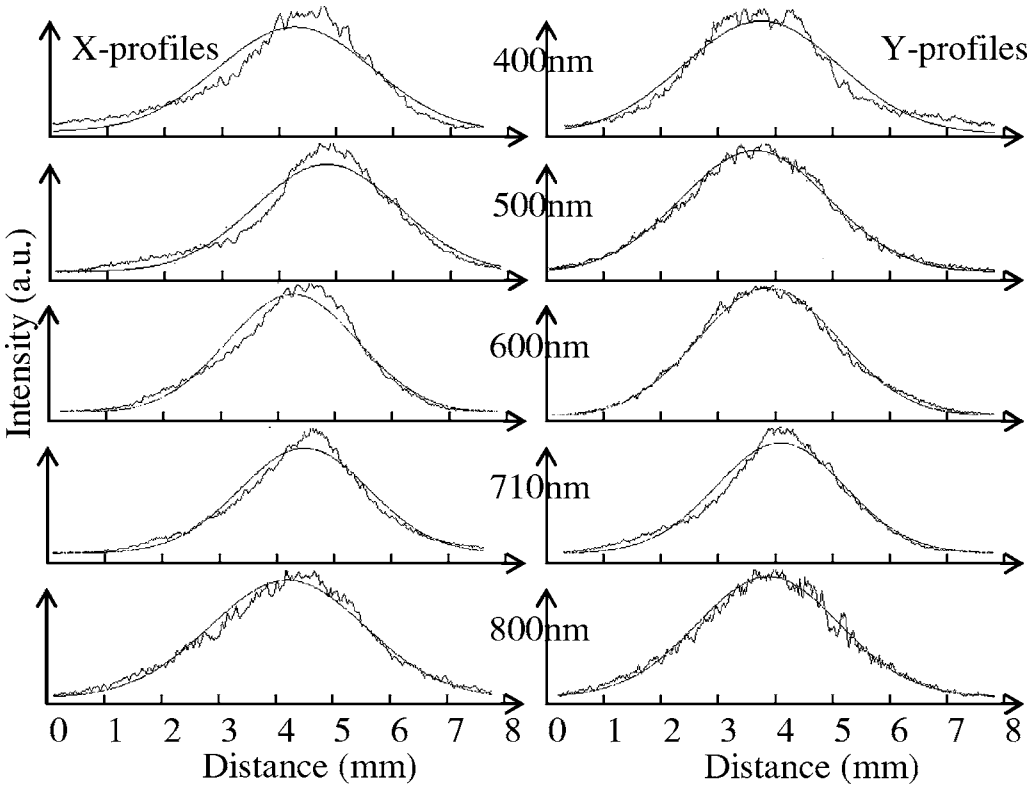

Fig. 3. Beam profiles corresponding to different wavelengths of the continuum.

ric autocorrelation is measured using the GaP detector. The results are shown in Fig. 4.

We notice the pulse widths have an average value at ~100 fs (FWHM in irradiance) for all the wavelengths transmitted by the NBFs except toward the blue where there is apparently a small increase in pulse width which may be related to the larger bandwidths and chirping of the pulses. For the longer wavelengths the ~100 fs and ~10 nm bandwidth transmitted by the NBF results in a time-bandwidth product of ~0.47, indicating nearly transform-limited pulses. However, the bandwidths of the NBFs are larger for the shorter wavelength filters allowing chirp on the pulses as shown by the time-bandwidth product values shown in Fig. 4(b). This was confirmed looking at interferometric autocorrelations, which showed almost no chirp for 690 nm and small but easily measurable chirp for 620 nm.

4. Z-SCAN EXPERIMENTAL SETUP

Figure 5 shows the WLC *Z*-scan experimental setup. The NBFs are mounted on a computer controlled filter wheel. Separation of the wavelengths is necessary prior to the sample to eliminate frequency nondegenerate nonlinearities [16].

In our previous work [1,2], we used ZnSe as a reference sample to test our setup since it is a well-characterized material [4–6]. Accordingly we also checked the present system with ZnSe but also made measurements on the wider bandgap material ZnS with ($Eg = 3.54$ eV versus $Eg = 2.7$ eV for ZnSe), which allows us to perform 2PA and nonlinear refraction measurements at shorter wavelengths (as short as 400 nm). We simultaneously measure

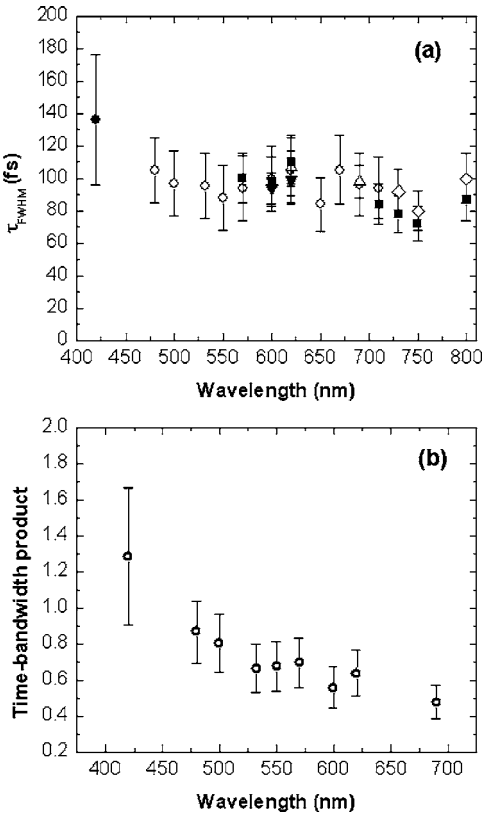

Fig. 4. (a) Pulsewidth measurement results for different wavelengths in the continuum transmitted by the NBFs. The autocorrelation is performed using: ●, a ZnS crystal and a Si detector; ○, a ZnSe crystal and a Si detector; ■, a GaP detector; ▼, a GaP detector with 100× gain; △, a GaP detector in an interferometric setup; and ◇, Grenouille (b) time-bandwidth product.

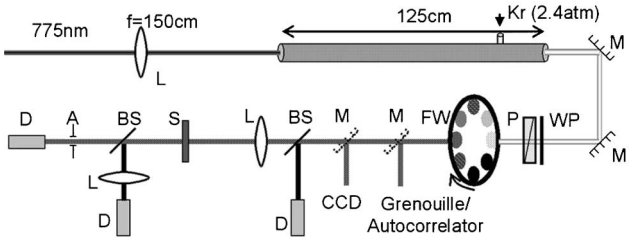

Fig. 5. WLC *Z*-scan experimental setup: L: lens; M: mirror; WP: half-wave-plale; P: polarizer; FW: filter wheel; BS: beam splitter; D: detector; A: aperture; S: sample; the dotted Ms are removable mirrors for beam characterization.

2PA and the corresponding nonlinear refraction dispersion by taking "open" and "closed" aperture *Z*-scan data at the same time for each spectral component transmitted by the filter wheel. This is shown in the lower left corner of Fig. 5.

The main advantage of this experimental setup over our previous ones [1,2] is that the continuum source has sufficient spectral energy density for performing *Z* scans on low nonlinearity samples including low concentrations of organic dye solutions as shown in Section 5.

5. EXPERIMENTAL RESULTS

A. Two-Photon Absorption and Nonlinear Refraction Results on ZnSe and ZnS

To verify the validity of the method, we demonstrate measurements of 2PA and n_2 on polycrystalline samples of the well-characterized semiconductors, ZnSe and ZnS. The thickness of the ZnSe sample is 0.5 mm and that of ZnS is 1 mm. A 30 cm focal length lens is used for focusing into the sample. The diffraction length in air, z_0, corresponding to this focusing geometry, varies over a range from 1.5 to 4 mm for the wavelengths between 400 and 800 nm.

The values of z_0 for different wavelengths assures a low limit for the linear diffraction in the sample required by the "thin sample approximation" [4]. The thickness of the samples is also important to determine the group-velocity dispersion (GVD) induced pulse-width broadening in the samples. We determine that pulse-width broadening needs to be accounted for at short wavelengths (shorter than 550 nm for ZnSe and shorter than 480 nm for ZnS). The largest GVD-induced broadening corresponds to 480 nm for ZnSe (from 100 to 128 fs) and to 400 nm for ZnS (from 136 to 157 fs), which are the shortest wavelength measurements taken for ZnSe and ZnS, respectively.

The values of the 2PA coefficient, β, and n_2 for ZnSe obtained from fits at different wavelengths [4,17] are presented in Fig. 6 along with the theoretical predictions of Refs. [5,6]. For this sample, on the blue side of the spectrum we are limited by the linear absorption of the sample while on the red side we are limited by the continuum range. Note the change in sign of n_2 at ~650 nm.

As mentioned above, we also examine a wider bandgap semiconductor for which we can measure 2PA and n_2 over the entire useful spectral range of the continuum, i.e., 400 to 800 nm. *Z*-scan experimental curves for the ZnS sample, along with their corresponding fittings [4,17] are presented in Fig. 7 for several wavelengths.

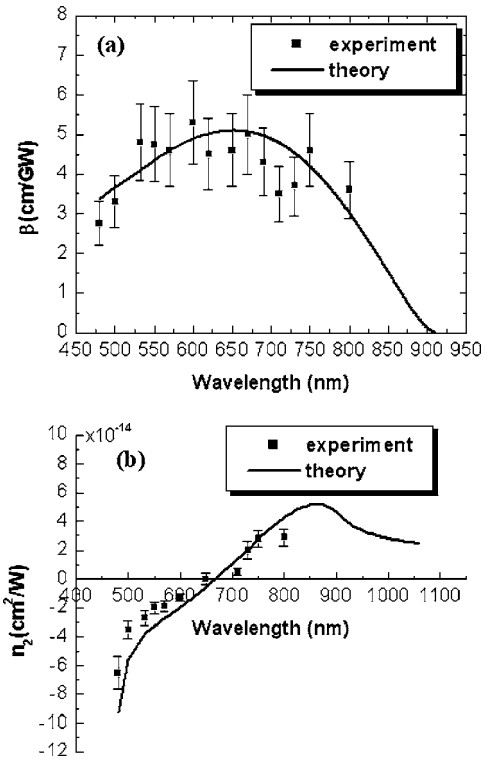

Fig. 6. (a) 2PA and (b) n_2 coefficients of ZnSe obtained from theory and from the experimental data fitting.

The values of β and n_2 corresponding to ZnS obtained from fits at different wavelengths are compared with the theoretical predictions of Refs. [5,6] and presented in Fig. 8.

We notice a reasonable agreement between experimental results and theoretical calculations for the 2PA spectrum and n_2 dispersion [4–6] corresponding to both ZnSe and ZnS as shown in Figs. 6 and 8 above, attesting to the usefulness of this technique.

B. Two-Photon Absorption and Nonlinear Refraction Results on Organic Materials (SJZ-316 and SY-242)

We also study nonlinearities of a 2.3×10^{-3} M solution of the organic dye 1 (see Fig. 9), which is compound 4 of [18] *E*,*E*,*E*-1,2-bis(3,4-di-*n*-butoxy-5-[4-{di-(4-methoxyphenyl)amino}styryl]thien-2-yl)ethene, an extended electron-rich chromophore quadrupolar dissolved in tetrahydrofuran (THF) and of a 5×10^{-3} M solution of organic dye 2 (see Fig. 10), 4-((*E*)-2-(7-(4-(benzo[*d*]thiazol-2-yl) styryl)- 9,9-didecyl-9H-fluoren-2-yl) vinyl) -*N*, *N*-dibutylaniline (SY-242), dissolved in cyclohexane.

Figure 9 compares the 2PA cross section of sample 1 measured by WLC *Z* scan with the results measured by single wavelength *Z* scans and two-photon excited fluorescence [18]. Also, in Fig. 9, we show the dispersion of the nonlinear refraction for this sample and compare the results with those measured by single wavelength *Z* scan. Both results show good agreement confirming the usefulness of the WLC-*Z*-scan technique for measuring low nonlinearities (the effective 2PA coefficient for this solution is $\sim10^{-2}$ cm/GW and the effective nonlinear refractive index

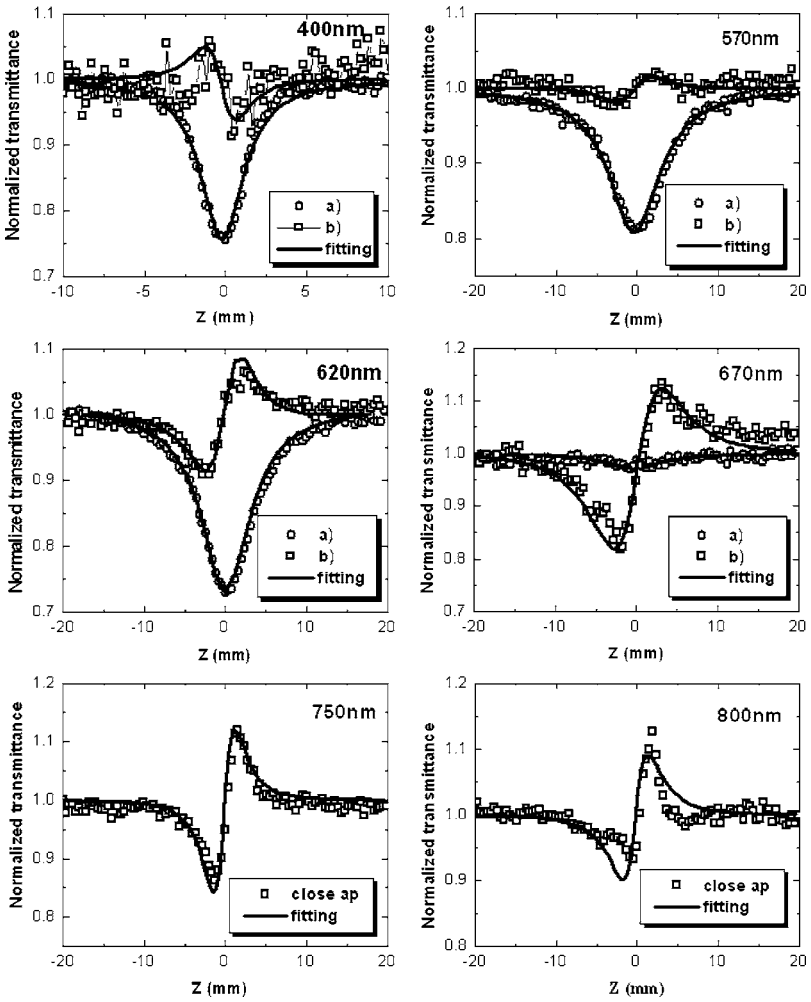

Fig. 7. *Z*-scan data for 1 mm thickness ZnS sample at 400, 570, 620, 670, 750, and 800 nm (a) open and (b) closed aperture (the result of the division with open aperture). The last two graphs do not show open aperture curves as 2PA was not present at those wavelengths.

is $\sim 10^{-16}$ cm^2/W. The nonlinear refraction is presented as a cross section defined as follows:

$$\delta_r = \frac{\hbar\omega}{N} k n_2,$$

where k is the wave number, N is the molecular concentration, and ω is the excitation frequency. Similar to the definition of the 2PA cross section, δ_r is also given in cm^4 s. Here we define a "refractive Göppert–Mayer" (RGM = 10^{-50} cm^4 s), to make it analogous to the absorptive case. In this way one can easily compare the refractive and absorptive parts of $\chi^{(3)}$, and the ratio δ_r/δ is a useful, unitless figure of merit, e.g., for optical switching applications. For sample 1 this figure of merit is $\sim 10^{-3}$ or smaller in magnitude although the sign changes.

It is also important to point out in Fig. 9 that as with semiconductor samples a change in sign of n_2 occurs near the peak 2PA. This change in sign of n_2 occurs around the 2PA peak. The negative n_2 for wavelengths shorter than the peak and positive for longer wavelengths is explained by the Kramers–Kronig relations for nonlinear optics although here we have not measured the nondegenerate nonlinearities required for a rigorous interpretation [19].

Figure 10 shows the 2PA cross section (on a semilogarithmic scale) measured by the WLC *Z* scan for sample 2. The solid curve was generated by fitting the experimental data with a high-order polynomial function and meant to be a guide to the eye. The structure of this material is also presented in the figure. The lowest cross section we measured for this organic was ~200 GM at 670 nm; however, with the signal-to-noise ratio observed, we estimate that we are able to measure cross sections as low as ~50–60 GM for visible wavelengths. Nonlinear refraction measured for this sample was not distinguishable from the one measured in pure cyclohexane ($\sim 10^{-15}$ cm^2/W), considering the experimental noise, it indicates that the maximum absolute value for the nonlinear refraction cross section is 0.27 RGM. We use both the continuum and single wavelength *Z* scans from our optical parametric amplifier for this determination.

6. CONCLUSION

We generate a high-spectral-irradiance, high-quality supercontinuum source by focusing femtosecond pulses into a chamber filled with Kr gas. This source is optimized for performing *Z* scans over its spectrum—here the entire

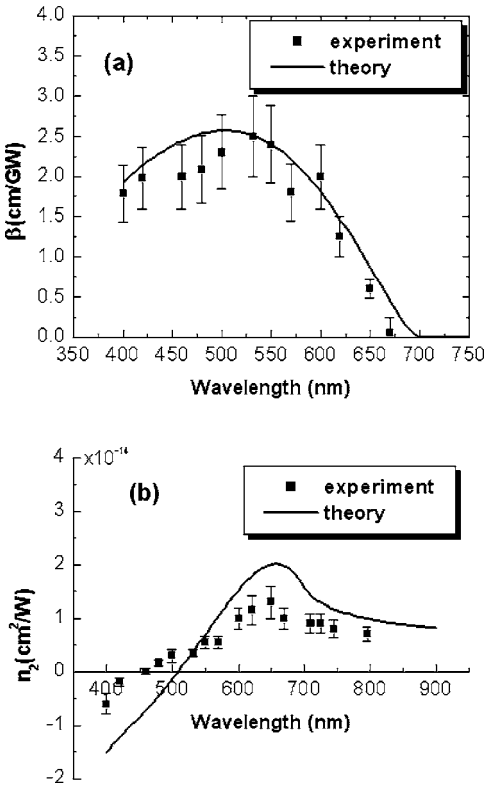

Fig. 8. (a) 2PA and (b) n_2 coefficients of ZnS obtained from theory and from the experimental data fitting.

visible range from 400 to 800 nm. We use this white-light continuum as the source in *Z*-scan experiments for rapid and simultaneous measurements of the spectrum of nonlinear absorption and the dispersion of nonlinear refraction. We experimentally verify the method on the well-characterized semiconductors ZnSe and ZnS. The good agreement between experimental results and theoretical calculations attests to the usefulness of this technique. We also show the method is sensitive enough for dilute solutions of organic dyes, which exhibit lower nonlinearities than semiconductors.

While this nonlinear spectrometer is already a beneficial tool for rapid nonlinear optical material characterization in our laboratory, we are working on finding a way to extend the spectral broadening of the WLC source. This will allow us to eventually eliminate the need for optical parametric sources for most of our measurements.

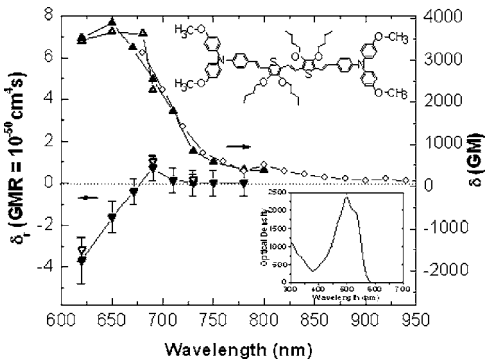

Fig. 9. 2PA spectrum and n_2 dispersion for sample 1 (upper right in figure). ○, 2PA measured by two-photon fluorescence; △, 2PA via single wavelength *Z* scan; ▲, 2PA via WLC *Z*-Scan; ∇, nonlinear refraction via single wavelength *Z* scan; ▼, nonlinear refraction via WLC *Z* scan. In the insets we show the linear absorption spectrum and the molecular structure [18].

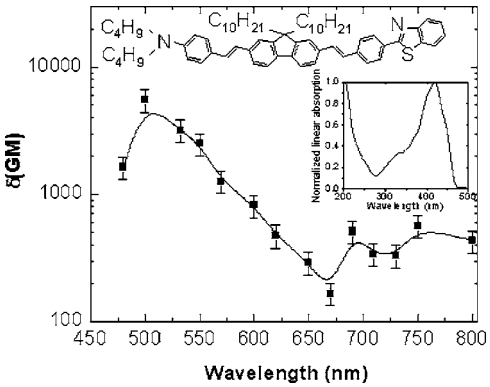

Fig. 10. 2PA cross-section spectrum for organic dye 2.

ACKNOWLEDGMENTS

We gratefully acknowledge the financial support of the National Science Foundation (NSF) (grant ECS 0217932), U.S. Air Force Office of Scientific Research (AFOSR) (contract FA95500410200), the U.S. Army Research Laboratory (contract W911NF0420012), and the U.S. Army Research Office (contract W911NF0610283). We thank Lauren Rich from the University of Missouri-Rolla for taking 2PA data. She acknowledges NSF Research Experience for Undergraduate support (grant EEC#0244033). Georgia Tech contributions are based upon work supported in part by the Science and Technology Center Program of the National Science Foundation under agreement DMR 0120968.

REFERENCES

1. M. Balu, J. Hales, D. J. Hagan, and E. W. Van Stryland, "White-light continuum *Z*-scan technique for nonlinear material characterization," Opt. Express **12**, 3820–3826 (2004).
2. M. Balu, J. Hales, D. J. Hagan, and E. W. Van Stryland, "Dispersion of nonlinear refraction and two-photon absorption using a white-light continuum *Z*-scan," Opt. Express **13**, 3594–3599 (2005).
3. P. B. Corkum and C. Rolland, "Supercontinuum generation in gases," Phys. Rev. Lett. **57**, 2268–2272 (1986).
4. M. Sheik-Bahae, A. A. Said, T. H. Wei, D. J. Hagan, and E. W. Van Stryland, "Sensitive measurement of optical nonlinearities using a single beam," IEEE J. Quantum Electron. **26**, 760–769 (1990).
5. E. W. Van Stryland, M. A. Woodall, H. Vanherzeele, and M. J. Soileau, "Energy bandgap dependence of two-photon absorption," Opt. Lett. **10**, 490–492 (1985).
6. M. Sheik-Bahae, D. C. Hutchings, D. J. Hagan, and E. W. Van Stryland, "Dispersion of bound electronic nonlinear refraction in solids," IEEE J. Quantum Electron. **27**, 1296–1309 (1991).
7. H. J. Lehmeier, W. Leupacher, and A. Penzkofer, "Nonresonant third order hyperpolarizability of rare gases and N2 determined by third harmonic generation," Opt. Commun. **56**, 67–72 (1985).
8. H. R. Lange, G. Grillon, J.-F. Ripoche, M. A. Franco, B. Lamouroux, B. S. Prade, and A. Mysyrowicz, "Anomalous long-range propagation of femtosecond laser pulses

through air: moving focus or pulse self-guiding?" Opt. Lett. **23**, 120–122 (1998).
9. A. Brodeur, C. Y. Chien, F. A. Ilkov, and S. L. Chin, "Moving focus in the propagation of ultrashort laser pulses in air," Opt. Lett. **22**, 304–306 (1997).
10. M. Mlejnek, E. M. Wright, and J. V. Moloney, "Dynamic spatial replenishment of femtosecond pulses propagating in air," Opt. Lett. **23**, 382–384 (1998).
11. M. Kolesik, E. M. Wright, A. Becker, and J. V. Moleney, "Simulation of third-harmonic and supercontinuum generation for femtosecond pulses in air," Appl. Phys. B **85**, 531–538 (2006)
12. R. Trebino, *Frequency Resolved Optical Gating: the Measurement of Ultrashort Laser Pulses* (Kluwer Academic, 2000).
13. D. T. Reid, M. Padgett, C. McGowan, W. E. Sleat, and W. Sibbett, "Lightemitting diodes as measurement devices for femtosecond laser pulses," Opt. Lett. **22**, 233–235 (1997).
14. S. Ross, "A picosecond visible OPO as a tool for non-linear spectroscopy," Ph.D. dissertation (University of Central Florida, 1998).
15. W. Rudolph, M. Sheik-Bahae, A. Bernstein, and L. F. Lester, "Femtosecond autocorrelation measurements based on two-photon photoconductivity in ZnSe," Opt. Lett. **22**, 313–315 (1997).
16. R. Negres, J. Hales, A. Kobyakov, D. J. Hagan, and E. W. Van Stryland, "Experiment and analysis of two-photon absorption spectroscopy using a white-light continuum probe," IEEE J. Quantum Electron. **38**, 1205–1216 (2002).
17. M. Sheik-Bahae, A. A. Said, and E. W. Van Stryland, "High-sensitivity, single-beam n_2 measurements," Opt. Lett. **14**, 955–957 (1989).
18. S. Zheng, L. Beverina, S. Barlow, E. Zojer, J. Fu, L. A. Padilha, C. Fink, O. Kwon, Y. Yi, Z. Shuai, E. W. Van Stryland, D. J. Hagan, J. L. Bredas, and S. R. Marder, "High two-photon cross-sections in bis(diarylaminostyryl) chromophores with electron-rich heterocycle and bis(heterocycle)vinylene bridges," Chem. Commun. (Cambridge), **13**, 1372–1374 (2007).
19. D. C. Hutchings, M. Sheik Bahae, D. J. Hagan, and E. W. Van Stryland, "Kramers–Kronig relations in nonlinear optics," Opt. Quantum Electron. **24**, 1–30 (1992).